High Resolution Velocity Analysis of Ocean Bottom Seismometer Data by the τ-p Method

MASANAO SHINOHARA[1], NAOSHI HIRATA[2], NARUMI TAKAHASHI[2]

[1] *Ocean Research Institute, the University of Tokyo, Tokyo 164, Japan*
[2] *Faculty of Science, Chiba University, Chiba 263, Japan*

(Received on January 28, 1993; accepted March 3, 1993)

Key words: Ocean Bottom Seismometer (OBS), direct τ-p mapping, τ-sum inversion, high resolution seismic structure

Abstract. A method of high resolution seismic velocity analysis for ocean bottom seismometer (OBS) records is applied to the study of the shallow oceanic crust, especially sedimentary and basement layers. This method is based on the direct τ-p mapping and the τ-sum inversion. We use data obtained from a 1989 airgun-OBS experiment in the northern Yamato Basin, Japan Sea and derive P- and S-wave velocity functions that can be compared with the seismic reflection profiles. Using split-spread profile records, we obtain interface dips and true interval velocities from the OBS data. These results show good agreement with the reflection profile records, the acoustic velocities of core samples, and sonic log profiles. We also present a method for estimating errors in the derived velocity functions by calculating covariance of the derived layers' thicknesses. The estimated depth errors are about 150 m at shallow depths, which is close to the seismic wavelength used. The high resolution of this method relies on accurate determination of shot positions by GPS, spatially dense seismic observations, and the use of unsaturated reflected waves arriving after the direct water wave that are observed on low-gain component records.

Introduction

Determination of seismic velocity structure from ocean bottom seismometer (OBS) records is commonly performed using the intercept-slope method or forward modeling using two-dimensional ray tracing (e.g., Červený *et al.*, 1977). Since these methods work in the time-distance domain, where refracted and reflected waves passing through shallow parts of the oceanic crust often arrive after the direct water waves, it is difficult to determine in detail shallow oceanic crust structures, especially sedimentary and basement layers.

In recent years, researchers have developed methods for seismic velocity analyses in the τ-p (intercept time-ray parameter) domain. The advantages of analysis in the τ-p domain compared to that in the X-T (distance-time) domain have been shown by many studies (e.g., Bessonova *et al.*, 1974; Henry *et al.*, 1980; Stoffa *et al.*, 1981; Kappus *et al.*, 1990). In the case of a one-dimensional structure, one advantage is that along each ray path the ray parameter is constant so that each trace in the τ-p domain represents a different plane wave; difficulties caused by X-T domain triplications are avoided because τ is a single-valued, monotonically decreasing function of p. Diebold and Stoffa (1981) and Stoffa *et al.* (1981) presented the direct τ-p mapping and the τ-sum inversion methods, and hereafter, we will call the velocity analysis consisting of these methods the "τ-p method":

Seismic traces in the X-T domain are mapped into the τ-p domain by the slant stacking (e.g., Stoffa *et al.*, 1981). The mapping for discrete finite aperture data is expressed by the summation

$$F(\tau_i, p_j) = \sum_{k=1}^{N} f(\tau_i + p_j X_k, X_k), \tag{1}$$

where $f(t_i, X_k)$ is the seismogram as a function of time, t_i, at a station with range X_k and N is the number of the seismic traces used in the mapping. The recursion which derives the velocity-depth function from discretely sampled τ-p data is the τ-sum inversion which is defined as

$$\left.\begin{aligned} h_1 &= \frac{\tau(p_2)/2}{(p_1^2 - p_2^2)^{1/2}} \\ h_i &= \frac{\tau(p_{i+1})/2 - \sum_{k=1}^{i-1} (p_k^2 - p_{k+1}^2)^{1/2} h_k}{(p_i^2 - p_{i+1}^2)^{1/2}} \\ & \qquad (i \geq 2) \end{aligned}\right\} \tag{2}$$

where h_i is the thickness of a layer with a velocity of $1/p_i$ (Diebold and Stoffa, 1981). Because these

Marine Geophysical Researches **16**: 185–199, 1994.

equations assume that the source and receiver are located at the same depth, they need to be modified for OBS data. For the OBS data if we measure depth from the seafloor, we have

$$\tau(p_n) = 2 \sum_{i=1}^{n-1} (p_i^2 - p_n^2)^{1/2} h_i + (c_0^{-2} - p_n^2)^{1/2} h_0, \tag{3}$$

where h_0 is the thickness of the sea water layer and c_0 is the P-wave velocity in the sea water. From Equation (3), we can see that Equation (2) can be used for the OBS data after replacing $\tau(p_i)$ in Equation (2) by

$$\tau(p_i) - (c_0^{-2} - p_i^2)^{1/2} h_0, \tag{4}$$

(Nishizawa and Suyehiro, 1986). Milkereit *et al.* (1985) presented a method for the τ-sum inversion in dipping planar structure. Diebold (1989) extended their method, using marine split-spread profile data, for two-dimensional structures with many planar interfaces of arbitrary dip.

The aim of the previous studies, which applied the τ-p method to OBS data, was to construct initial velocity models for ray tracing. In these studies, the focus was on relatively deep structures and the fine-scale resolution of the results was not discussed in detail. The τ-sum inversion method for identifying two-dimensional structure has not previously been applied to OBS data. In addition, recent technologic advances allow us to make spatially dense seismic observation using many OBS's, determine locations accurately using the Global Positioning System (GPS), and constantly increasing computer performance permits us to process the vast amount of data generated by these experiments. In this paper, we reformulate the τ-p method for OBS data to obtain high-resolution P- and S-wave velocity structures in oceanic crust, with special attention to defining sedimentary and basement layers, that can be compared to seismic reflection profiles. We also modify the τ-p method to obtain two-dimensional structure from OBS data and present a method for quantitatively estimating errors in the τ-p method.

The τ-p Method for OBS's: 1-D Structure

1. P-WAVE VELOCITY STRUCTURE

In this section, we present the τ-p method for a structure with horizontally homogeneous layers (1-D structure). This assumption is valid when the seafloor around the OBS is relatively flat. First, we perform the direct τ-p mapping. Second, discrete τ-p data are obtained by digitizing (picking up) the trajectory of refracted and postcritical reflected waves from the τ-p maps. Finally, a P-wave velocity-depth function, $V(d)$, is derived by the τ-sum inversion using the τ-p data. This procedure to obtain the $V(d)$ function is basically the same as previous studies, however, we modify the procedure to provide higher resolution results.

Following Stoffa *et al.* (1981), the direct τ-p mapping of OBS data is performed by calculating either the semblance (Neidell and Taner, 1971) or the slowness stack. In the τ-p mapping, semblance $S(\tau_i, p_j)$ is defined as

$$S(\tau_i, p_j) = \frac{\sum_W \left(\sum_{k=1}^{N} f(\tau_i + p_j X_k, X_k) \right)^2}{N \sum_W \sum_{k=1}^{N} (f(\tau_i + p_j X_k, X_k))^2}, \tag{5}$$

where W represents a time window centered about the linear X-T trajectory (Stoffa *et al.*, 1981). Since the τ-p trajectory is digitized from the τ-p map and we use the discrete τ-p data for the τ-sum inversion after digitizing the τ-p trajectory, we can use the τ-p maps by calculating either slowness stack or semblance, which means that the wave form in the τ-p domain is not used for the inversion. We digitized the τ-p trajectory from τ-p maps transformed using semblance, since the τ-p maps made using semblance exhibit high amplitudes for arrivals with even modest signal-to-noise ratios (SNR's) and suppress spatial aliasing. An additional reason to use semblance for the direct τ-p mapping is because of the relatively low frequency and a small dynamic range of analog recording OBS data.

Due to the small dynamic range per channel in analog recording OBS's, we usually use a low-gain vertical component, that can clearly record waves reflected from basement, at offsets up to 10 km to identify shallow structures and a high-gain vertical channel, suitable for recording high amplitude refracted waves, for 10 to 20 km to derive deeper structures for the direct τ-p mapping. It is important that unsaturated reflected waves, arriving after the direct water wave and recorded on a low-gain component are used to permit the high resolution analysis.

Accurate positioning of sources and OBS's is also important for producing τ-p maps with high quality. The relative position between the source and the OBS must be accurate enough for effective

slant stacking, therefore, GPS is used for ship navigation. The ship positions at which the controlled sources were fired is determined by interpolating the GPS fixes. In general, the accuracy in source positions is estimated to be about 20 m. The seafloor position of the OBS is determined using the direct water wave travel times for shots within 10 km of the OBS. We estimate that this procedure allows us to locate the instrument positions to within a few tens of meters.

In 1989, an airgun-OBS experiment was carried out in the northern Yamato Basin, Japan Sea (Shinohara *et al.*, 1992). The data collected in this experiment are suited for the application of the τ-p method. A 1000-in^3 airgun was shot every 150 m along an E-W profile over the OBS. The data were recorded by direct analog recording OBS's. After the cruise, the analog data were digitized using a sampling frequency of 100 Hz. Figure 1 shows seismic record sections in the X-T domain. The reflected waves from basement are clearly seen on the low-gain channel records (Figure 1a), and the first arrivals can be seen at offsets to at least 20 km on the high-gain channel records (Figure 1b). Figure 2 shows the same records mapped into the τ-p domain using semblance with a window of 0.1 s. The τ-p maps were constructed by using the low-gain channel records (Figure 1a) at offsets from 0 to 10 km to see the reflected waves from basement (Figure 2a). The other τ-p maps were also constructed to enhance the deeply penetrating refracted waves (Figure 2b). The τ-p maps in Figure 2b were transformed using the high-gain channel records (Figure 1b) at offsets from 10 km to 20 km.

Figure 3 shows the discrete τ-p data for the P-wave τ-p trajectory of refracted and postcritical reflected waves. The τ-p data were obtained by digitizing the τ-p trajectory from the τ-p maps shown in Figure 2. The τ-p data labeled R1 and R2 were picked from the low-gain channel τ-p map and the high-gain channel τ-p map, respectively. We used the τ-p data shown in Figure 3 for the τ-sum inversion. Because we analyzed the eastward records and the westward records separately, we obtained two series of τ-p maps, which are shown in Figure 2, and two τ-p datasets shown in Figure 3.

Figure 4 shows P-wave $V(d)$ functions (thin lines) derived from the digitized discrete τ-p data shown in Figure 3. Our OBS was deployed at the same location as ODP Leg 128 Hole 794D. In Figure 5, our P-wave $V(d)$ functions are compared to ODP Leg 128 Site 794 shipboard P-wave velocity analyses of core samples and in situ velocities measurement by sonic logging (Shipboard Scientific Party, 1990a, b). Although the wave length of data recorded by the OBS is about 1000 times greater than that used in core sample (50 kHz) or sonic logging (20 kHz) measurements, the velocity functions derived by the τ-p method are similar to those obtained from the core samples and sonic logging.

Conversion of these velocity functions into two way travel time, $V(t)$ reveals a large increase in velocity from 1.7 to 4.5 km s^{-1} just below 0.75 s below the seafloor. Comparison between the $V(t)$ functions and a seismic reflection profile across the OBS and the drill hole shows that this velocity increase corresponds to the observed acoustic basement at 4.5 s in the reflection profile (Figure 6) and drilled at ODP Site 794.

2. S-WAVE VELOCITY STRUCTURE

There are several difficulties in deriving S-wave structures using the τ-p method. Constraints arise from the fact that P- to S-wave or S- to P-wave conversion may occur at interfaces within the crust. Since we infer that these conversions are most effective at the sediment-basement interface, where the velocity contrast is large, it is difficult to derive the S-wave velocity structure in sedimentary layers due to the principle of the t-sum inversion method.

In its original, simple form, the τ-sum inversion method assumes that the velocity function always increases with depth. The τ-sum inversion method for S-wave structure is carried out under the assumption that the S-wave velocity just below the top of basement is greater than P-wave velocity in the sedimentary layers. If the opposite is true, the thickness of first derived layer in the S-wave structure is thinner than its true thickness; errors in the depths of the S-wave velocities become large. A phase which propagates as a P-wave in sedimentary layers and an S-wave in the igneous crust (PSP phase) must be observed to allow for the τ-sum inversion of S-wave structures (Figure 7). Because the PSP phase propagates as a P-wave in the sedimentary layers, the τ-sum inversion can be performed without S-wave velocities in sedimentary layers as initial values for the inversion.

After the trajectory of a PSP phase is picked from the direct τ-p map, an S-wave $V(d)$ function is derived by Equation (2). However, $\tau(p_i)$ of Equation (2) must be replaced by

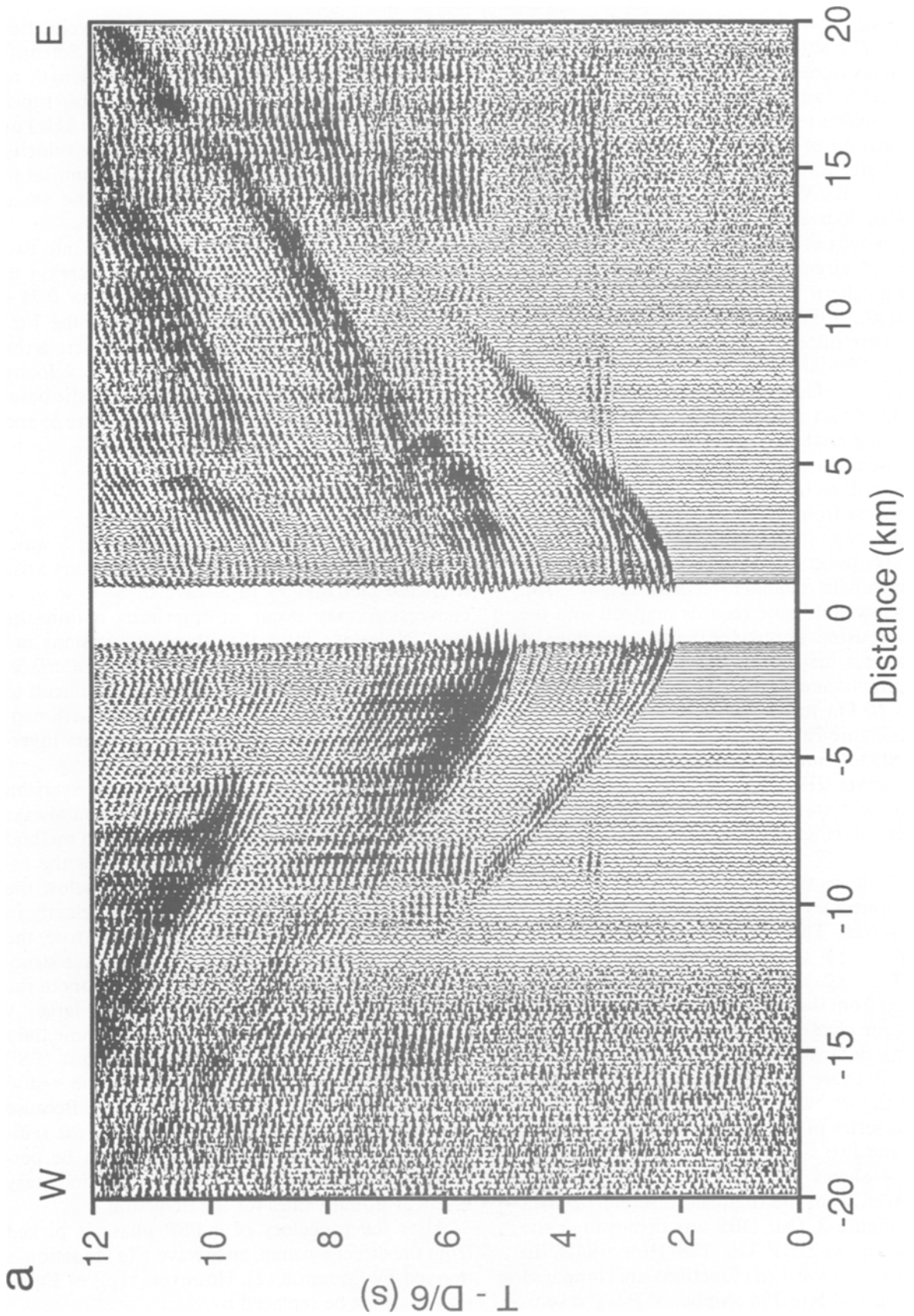

Fig. 1a.

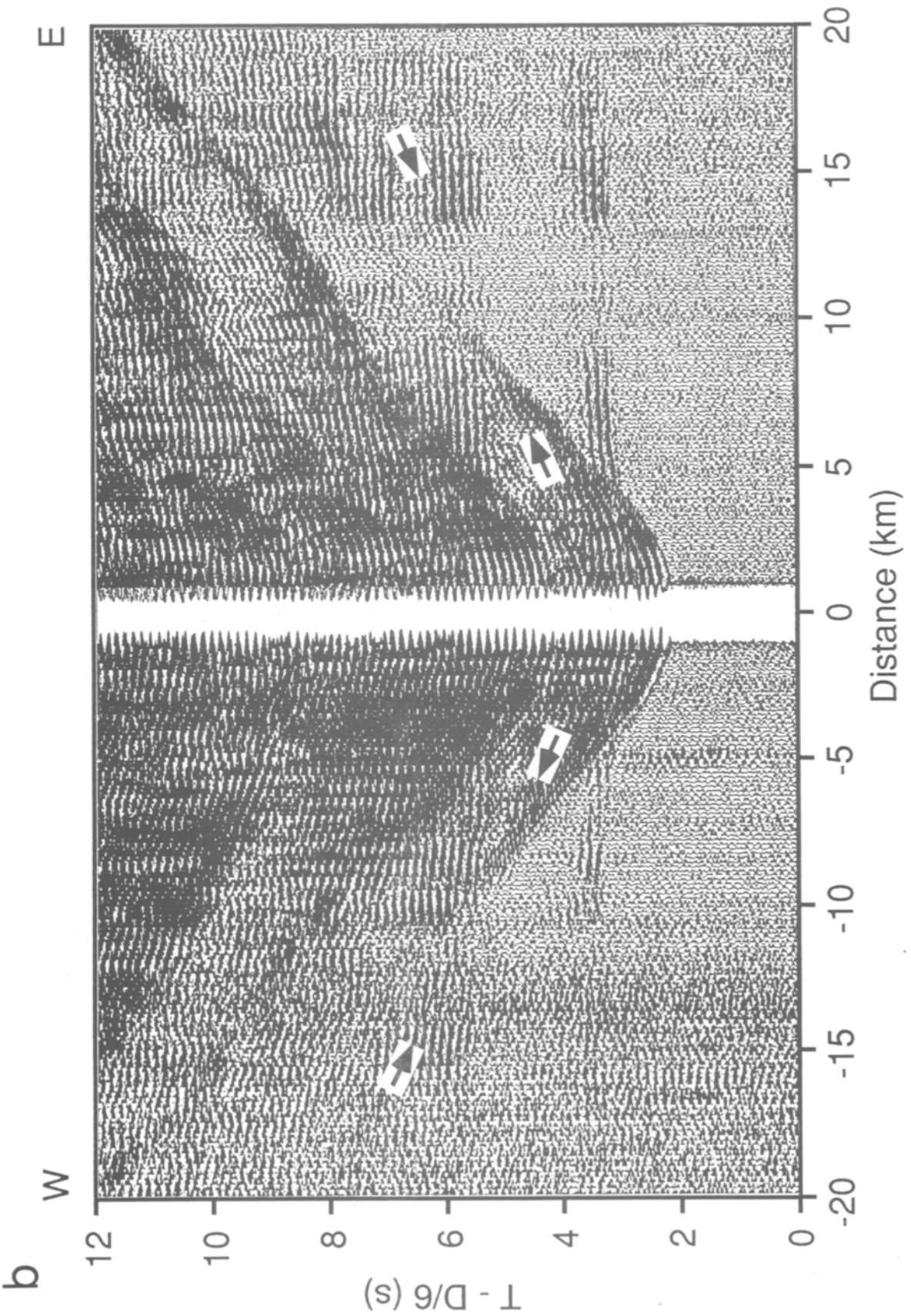

Fig. 1. Examples of analog recording OBS data in the X-T domain. The data were obtained during a 1989 airgun-OBS experiment in the northern Yamato Basin, Japan Sea. The profile trends east to west. Reduction velocity is 6.0 km s^{-1}. Band-pass filtering is 5–15 Hz. Each trace is normalized by its maximum amplitude. (a) Record section for a vertical component, low-gain channel. (b) Record section for a vertical component, high-gain channel. Arrivals of the PSP-phase on both the east side and the west side are shown by arrows.

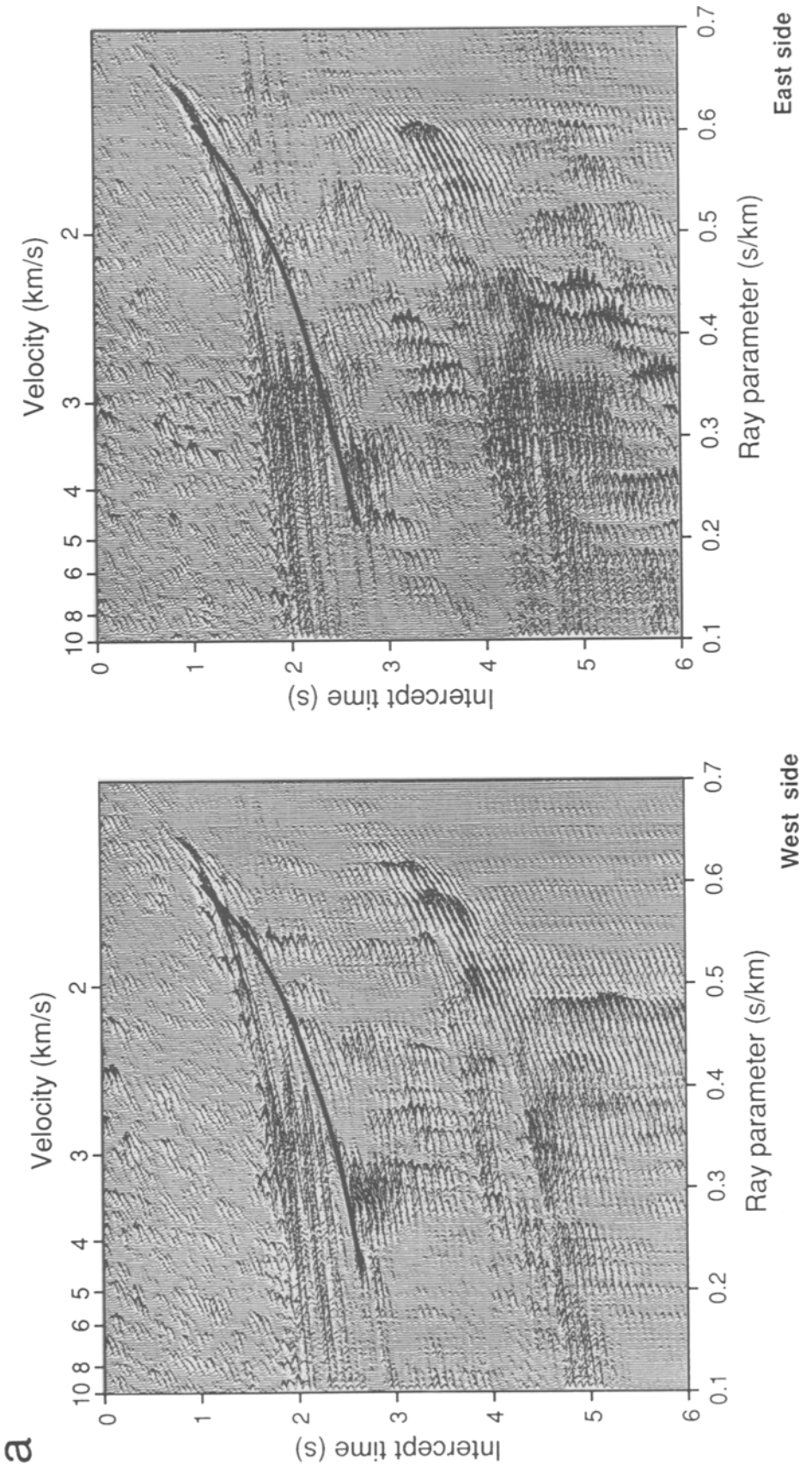
a
Velocity (km/s)
10 8 6 5 4 3 2
Intercept time (s)
0 1 2 3 4 5 6
Ray parameter (s/km)
0.1 0.2 0.3 0.4 0.5 0.6 0.7
West side
East side

Fig. 2a.

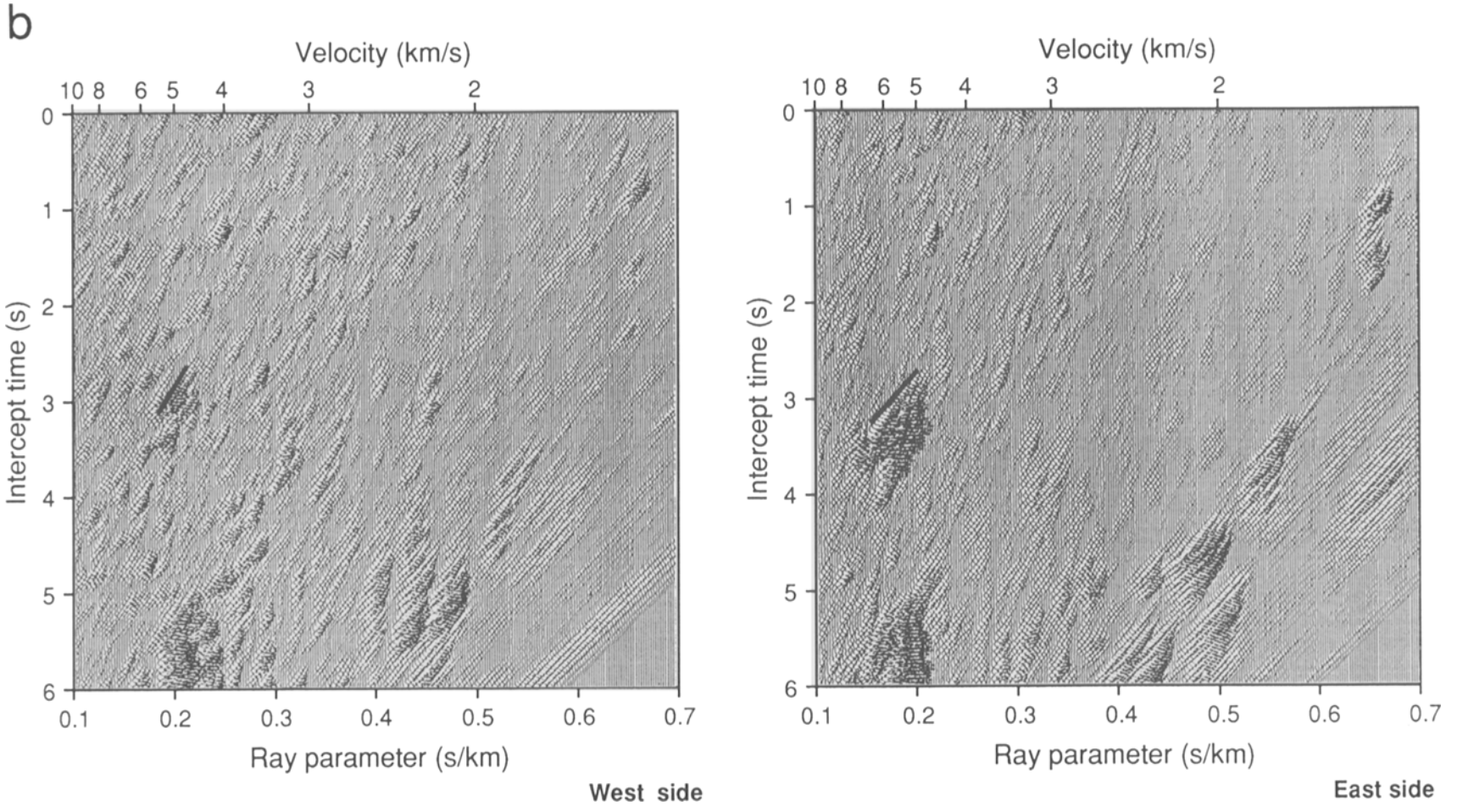

Fig. 2. Examples of OBS data in the τ-p domain, obtained during a 1989 airgun-OBS experiment in the Japan Sea. The τ-p mapping was performed by calculating semblance. (a) OBS data in the τ-p domain transformed using the vertical component low-gain channel records for offsets up to 10 km. Solid lines indicate the trajectory of reflected waves from basement. Two τ-p maps derived from records on either side of the OBS (east side–right, west side–left) are shown. (b) OBS data in the τ-p domain transformed using the vertical component high-gain channel records for offsets from 10 km to 20 km. Solid lines indicate the trajectory of deeply penetrating refracted waves. Two τ-p maps derived from records on either side of the OBS (east side–right, west side–left) are also shown.

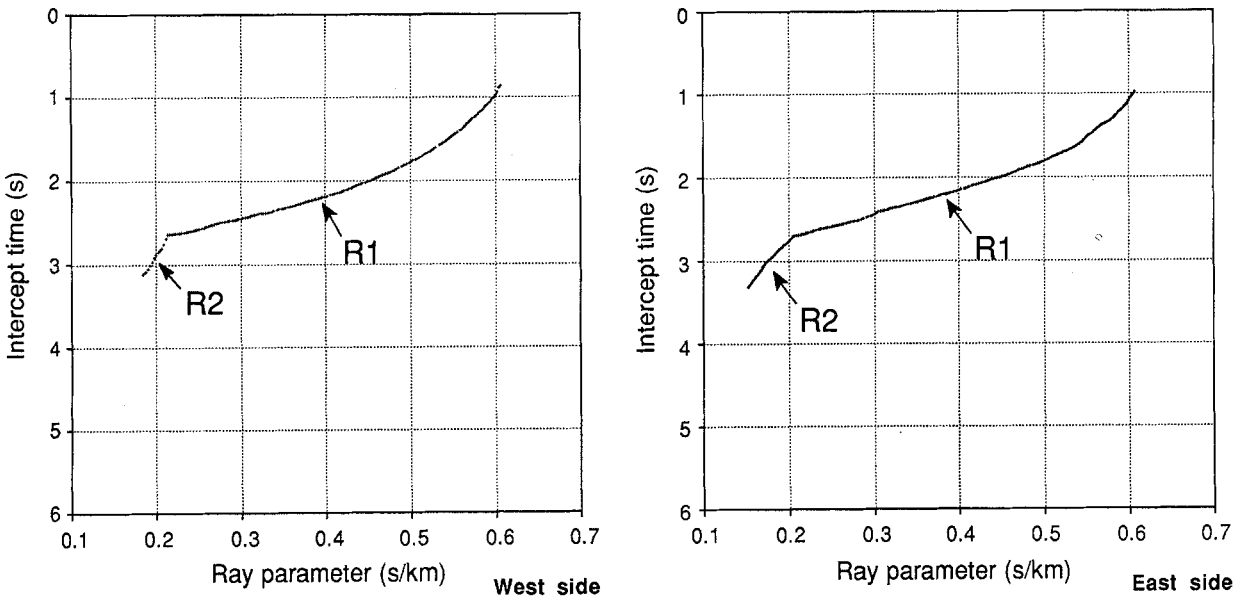

Fig. 3. Discrete τ-p data obtained by digitizing (picking up) the P-wave τ-p trajectories of refracted and postcritical reflected waves in Figure 2. The τ-p data labeled R1 and R2 were obtained from the low-gain channel τ-p maps (Figure 2a) and the high-gain channel τ-p maps (Figure 2b), respectively. The τ-p data R2 are essential for determining deeper structures. The two τ-p datasets; one was derived from the eastward records (right) and the other was derived from the westward records (left), are shown.

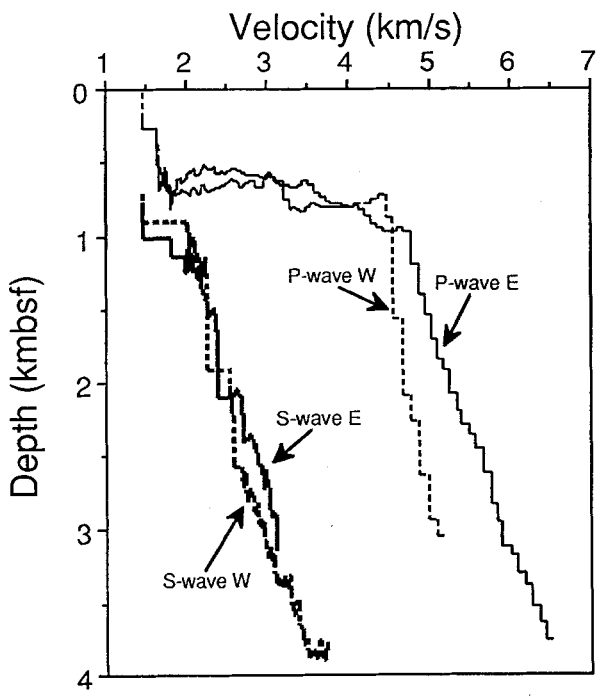

Fig. 4. P-wave (thin lines) and S-wave (thick lines) velocity functions of depth obtained for the profile on either side of the OBS shown in Figure 1. Solid and dashed lines are derived from the eastward and westward records, respectively. Depth is measured from the seafloor. S-wave velocity functions with velocities greater than the sediment P-wave velocity are obtained.

$$\tau(p_i) - (c_0^{-2} - p_i^2)^{1/2} h_0 - 2 \sum_{j=1}^{m} (c_j^{-2} - p_n^2)^{1/2} h_j, \quad (6)$$

where m is the number of sedimentary layers and c_j is the P-wave velocity of j-th sediment layer.

In the 1989 airgun-OBS experiment, PSP phases were observed in the same OBS (Figure 1b). Figure 8 shows the τ-p maps using semblance with a window of 0.1 s. The τ-p maps were constructed by using the high-gain channel records (Figure 1b) at offsets from 5 to 15 km to enhance the PSP phases. Figure 9 shows the discrete τ-p data obtained by digitizing the PSP-phase τ-p trajectory.

The S-wave $V(d)$ functions, derived using the τ-p data in Figure 9, are shown in Figure 4 (thick lines). The S-wave $V(d)$ functions start just beneath the top of basement due to the assumption discussed above. We modeled the sediment as a layer ($m = 1$) of 0.57 km thick with a P-wave velocity of 1.81 km s^{-1}. This model is based on the P-wave $V(d)$ functions also derived by the τ-p method (thin lines, Figure 4).

The τ-p Method for OBS's: 2-D Structure

The 1-D structure derived by the τ-p method assumes a stack of homogeneous layers. When dip-

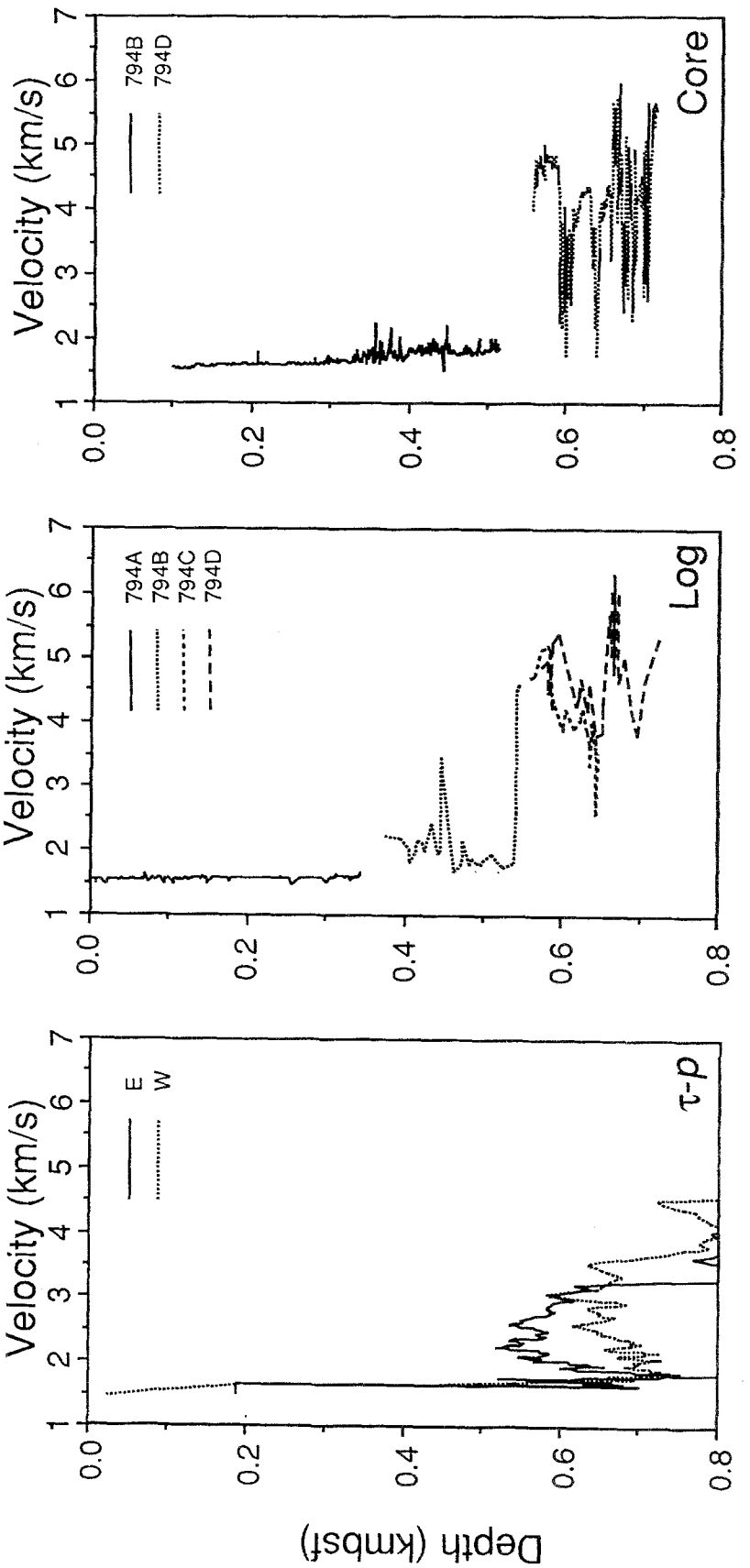

Fig. 5. Comparison of the acoustic velocities obtained from ODP Site 794 core sample (right) and sonic logging data (middle) with results of the τ-*p* method (left). Site 794 is located in the same position as the OBS whose data is shown in Figures 1 and 2. The *V(d)* functions derived by τ-*p* method are similar to the core sample and sonic logging velocity measurements.

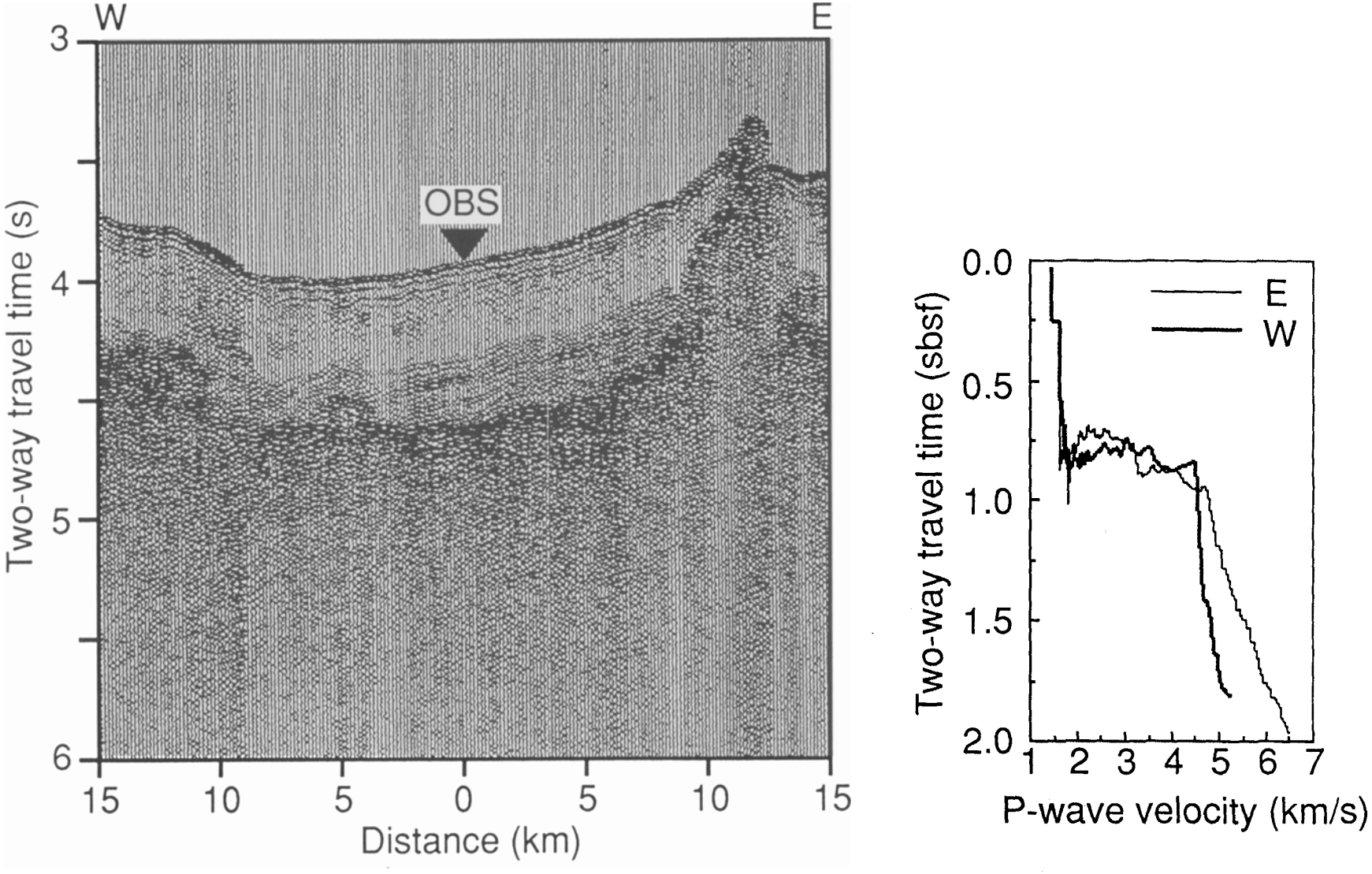

Fig. 6. Comparison of a seismic reflection profile with the τ-*p* method results. The *V(d)* function shown in Figure 2 has been converted to two-way travel time measured from the seafloor. The position of the OBS is marked on the seismic profile. Note the rapid increase in P-wave velocity at the acoustic basement.

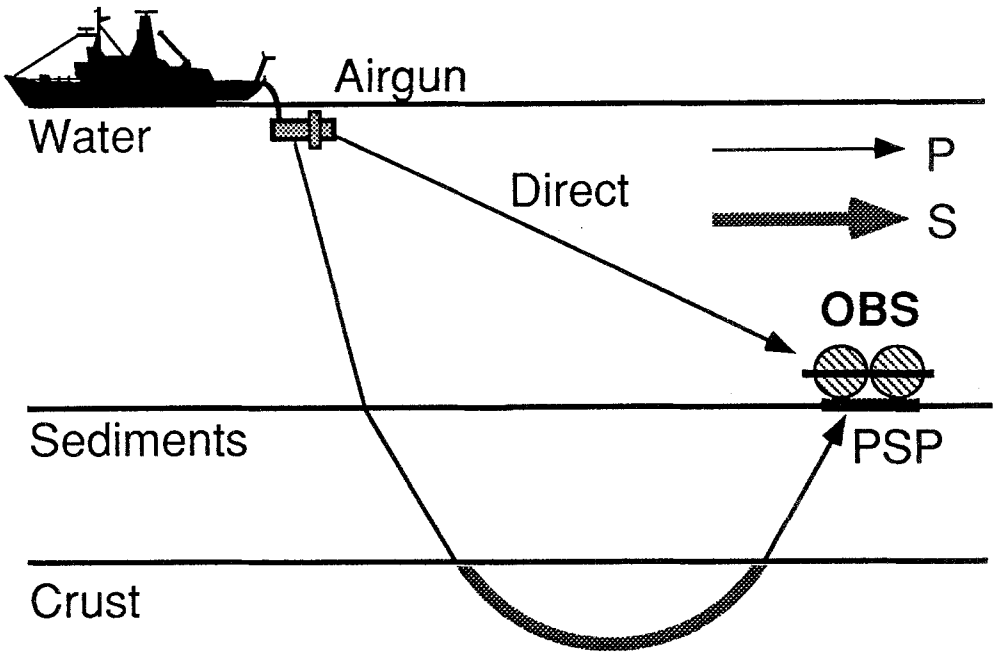

Fig. 7. Schematic diagram showing the PSP phase ray path, which is often observed on OBS seismograms and is convenient for the τ-sum inversion to obtain S-wave velocity functions.

ping interfaces separate the homogeneous layers, we can use two $V(d)$ functions derived from records from either side of the OBS using the τ-p method described in the previous section (Figure 4, east side–E, west side–W) to determine layer dips. Differences between the two $V(d)$ functions are inferred to represent the dip of the interface. Because the eastward $V(d)$ function indicates higher velocity than that on the west for the same depth (> 1 km, Figure 4), the interface dips to the west.

If we assume that lateral inhomogeneities exist only in the form of the dipping interfaces between homogeneous layers, we can quantitatively estimate interface dips and layer velocities from the split-spread profile records. The notations we will use in this section are the same as those presented in Diebold (1989). During OBS profiling, the OBS remains in a fixed position while the source moves from one side of the OBS to the other. We define the negative (p_a) and positive (p_b) ray parameters to represent either side of the OBS. When dipping layers are encountered the observed ray parameters, p_a and p_b, are not coincident for a given intercept time, τ. True velocities, layer thicknesses and interface dips are determined from the top down using $\tau(p_a)$ and $\tau(p_b)$ picks. First, true velocities and dips are obtained, and then layer thicknesses are determined by the τ-sum recursion (Diebold, 1989).

We modify Diebold's method for the geometry of OBS profiling under the assumption that a velocity of the layer just beneath the seafloor is the same as that of sea water. We see that the inversion procedure for 2-D structure can be used for OBS data after replacing $\tau(p_a)$ and $\tau(p_b)$ of Diebold (1989) by

$$\left.\begin{aligned}\tau_a^*(p_a) &= \tau(p_a) - Z_0(u_0^{-2} - (p_a)^2)^{1/2} \\ \tau_b^*(p_b) &= \tau(p_b) - Z_0(u_0^{-2} - (p_b)^2)^{1/2}\end{aligned}\right\}, \qquad (7)$$

where Z_0 and u_0 represent the water depth and the sea water P-wave velocity, respectively; i.e., reduce τ to the seafloor. Because p_a and p_b are different in the case that both $\tau(p_a)$ and $\tau(p_b)$ are coincident, $\tau_a^*(p_a)$ and $\tau_b^*(p_b)$, which are calculated using Equations (7) become different. Therefore, for this inversion procedure requires re-picking $\tau_a^*(p_a)$ and $\tau_b^*(p_b)$, with $\tau_a^*(p_a) = \tau_b^*(p_b)$. We calculate a new set of $\tau_a^*(p_a)$ and $\tau_b^*(p_b)$ using interpolation. After this procedure, dips and velocities of layers are derived by the first inversion step. Finally, layer thicknesses can be calculated using Equations (13) in Diebold (1989).

The dips and true velocities derived from the same OBS records in the previous examples are shown in Figure 10. The angle is measured counterclockwise from the horizontal viewed from the south, i.e., positive angles dip to the west. The true velocity is between those derived from either side of the profile. The sedimentary layers are nearly

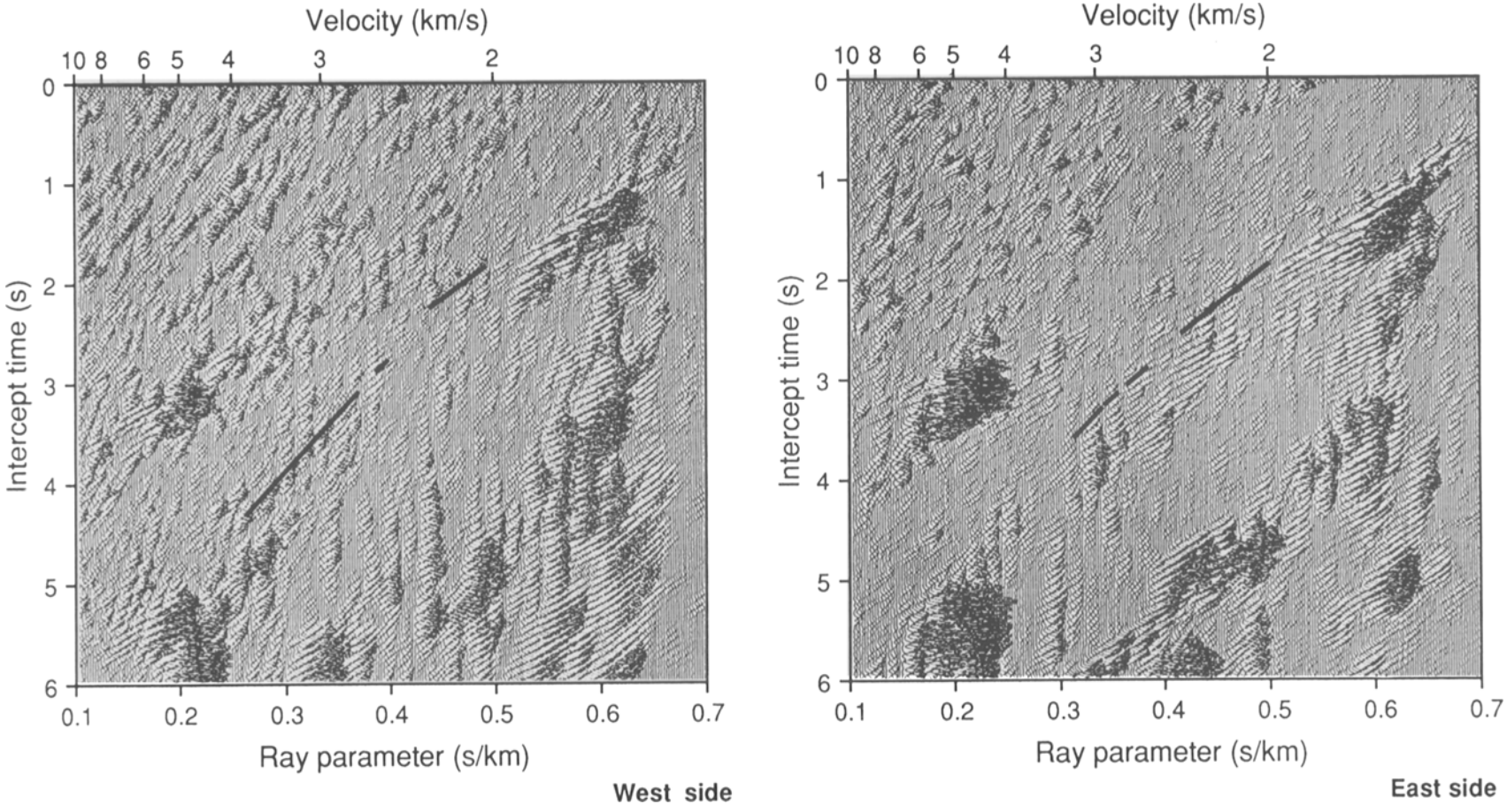

Fig. 8. Examples of OBS data in the τ-p domain for determining S-wave velocity functions. The τ-p mapping was also performed by calculating semblance. OBS data in the τ-p domain transformed using the vertical component high-gain channel records for offsets from 5 to 15 km (Figure 1b). The range was chosen to enhance the PSP-phase. Solid lines indicate the trajectory of the PSP-phase. Two τ-p maps derived from records on either side of the OBS (east side–right, west side–left) are shown.

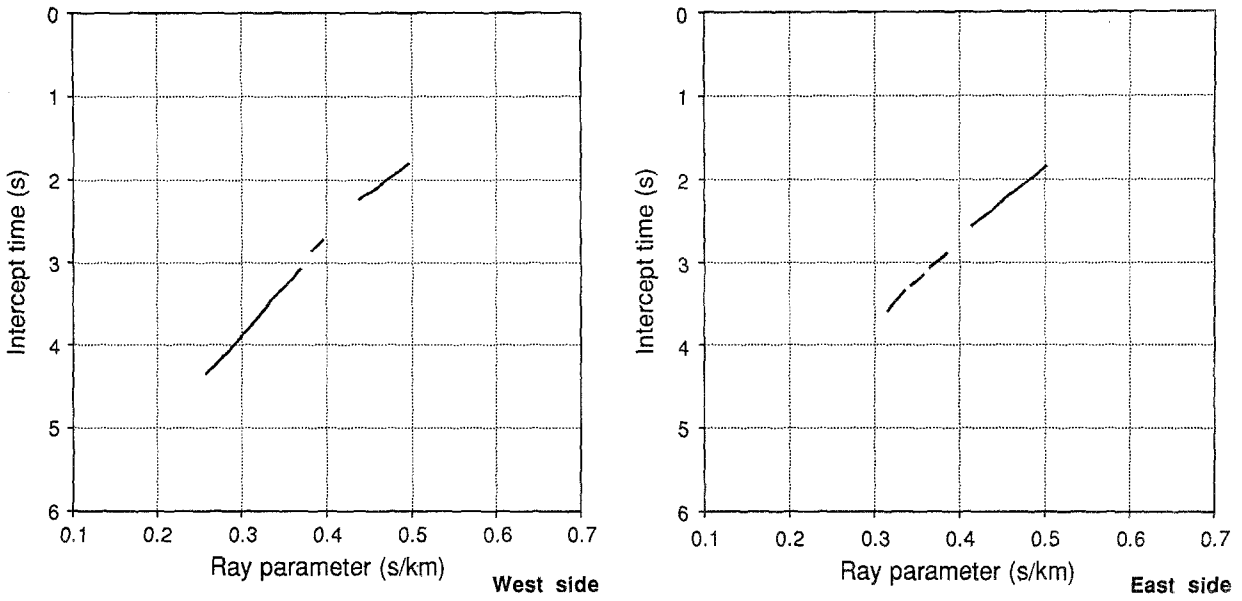

Fig. 9. Discrete τ-p data for deriving S-wave velocity functions by digitizing the PSP-phase trajectory in Figure 8. The two τ-p datasets; one was derived from the eastward records (right) and the other was derived from the westward records (left), are shown.

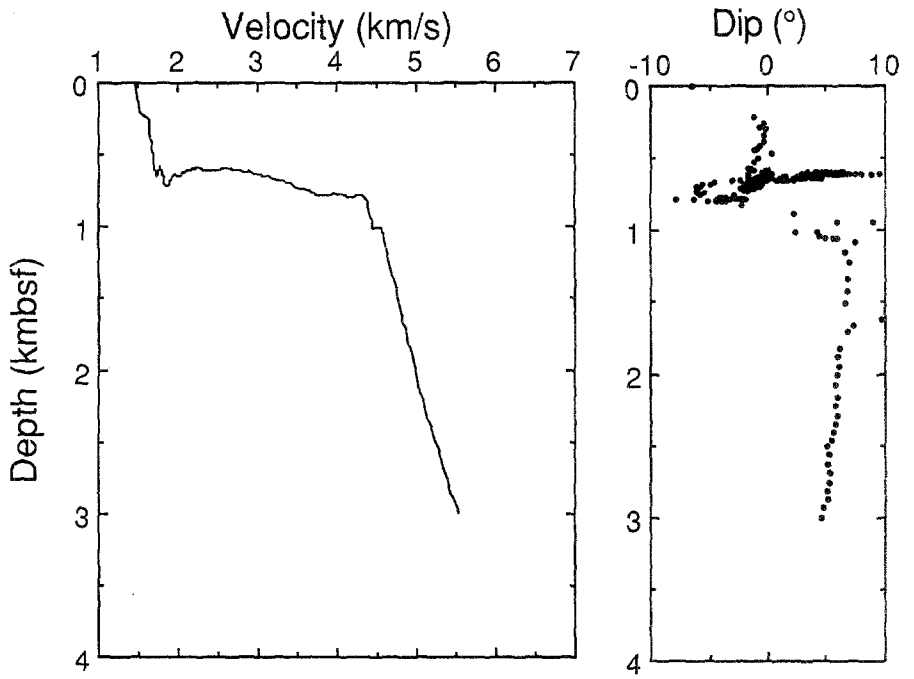

Fig. 10. Interface dips and true P-wave velocities in layers which are derived by a method modified for OBS data from Diebold (1989). The dip angle is measured counterclockwise from the horizon looking from the south. The sedimentary layers exhibit little dip and the basement layer dips 5° to the west. A true velocity just below the top of acoustic basement is estimated to be about 4.5 km s^{-1}.

horizontal and the basement layer dips 5° to the west. Large scatter in the dips at the top of the basement layer suggest large errors in the angle estimates. We also notice in Figure 10 that there is some deviation from linearity for the interface within the 0–10 or 15 km offset range.

Error Estimation of the τ-Sum Inversion

Few studies have quantitatively estimated errors in $V(d)$ functions derived by the τ-sum inversion. Since the depth estimate obtained by the τ-sum inversion method (Equations (2)) is a linear com-

bination of τ data, it is straightforward to derive a covariance matrix in terms of a covariance matrix of τ. Assuming that an observed τ_j of given p_j has a variance of $\sigma_{\tau_j}^2$ and is statistically independent of τ_k for $k \neq j$, we can estimate the errors in the $V(d)$ function by calculating the covariance matrix. The depth of a layer with a velocity of $1/p_m$ is expressed by

$$d_{m-1} = \sum_{j=1}^{m-1} h_j, \tag{8}$$

where h_j is the thickness of the j-th layer. To estimate the error in d_{m-1}, we calculate variance of d_{m-1}, $\sigma_{d_{m-1}}^2$, as

$$\sigma_{d_{m-1}}^2 = \sum_{j=1}^{m-1} \mathrm{cov}[h_j, h_j] + 2 \sum_{j=1}^{m-1} \sum_{j'>j}^{m-1} \mathrm{cov}[h_j, h_{j'}], \tag{9}$$

where $\mathrm{cov}[X, Y]$ represents covariance of X and Y. From Equation (2), the first term of Equation (9) is expressed by

$$\left.\begin{aligned} \mathrm{cov}[h_1, h_1] &= \frac{\sigma_{\tau_2}^2}{4q_2^2(p_1)} \\ \mathrm{cov}[h_j, h_j] &= \frac{1}{4q_j^2(p_{j+1})} \\ &\times \left\{ \sigma_{\tau_{j+1}}^2 + \sum_{k=1}^{j-1} 4q_k^2(p_{j+1}) \right. \\ &\left. \times \mathrm{cov}[h_k, h_k] \right\} \qquad (j \geq 2), \end{aligned}\right\} \tag{10}$$

with

$$q_k(p_j) = (p_k^2 - p_j^2)^{1/2}, \tag{11}$$

and σ_{τ_j} being a measurement error of the j-th data of τ. The second term of Equation (9) is expressed by

$$\begin{aligned} \mathrm{cov}[h_j, h_{j'}] &= \frac{1}{4q_j(p_{j+1})q_{j'}(p_{j'+1})} \\ &\times \left\{ \sum_{k=1}^{j-1} \sum_{m=1}^{j'-1} 4q_k(p_{j+1})q_m(p_{j'+1})\mathrm{cov}[h_k, h_m] \right. \\ &\left. - \sum_{k=1}^{j-1} 2q_k(p_{j+1})\mathrm{cov}[\tau_{j'+1}, h_k] \right\}, \\ &(j \geq j'+1), \end{aligned} \tag{12}$$

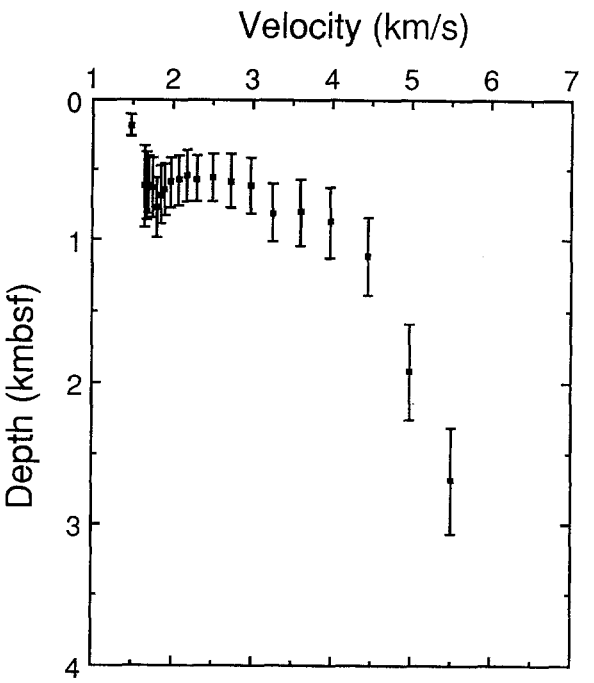

Fig. 11. Estimated errors in the P-wave $V(d)$ function derived by the τ-sum inversion of the records of the east side of the OBS (Figure 2). Length of the single-sided error bars corresponds to 1σ. The depth errors are a few hundred meters in the shallow section and 300 ~ 500 m in the deeper parts. The depth errors where velocity increases rapidly are large (i.e., top of basement), but then decrease with increasing velocity.

where $\mathrm{cov}[\tau_n, h_k]$ ($j'+1$ is replaced by n) is calculated as follows;

$$\left.\begin{aligned} &\mathrm{cov}[\tau_1, h_k] = 0 \qquad (k \geq 1) \\ &\mathrm{cov}[\tau_n, h_k] \\ &= \frac{1}{2q_k(p_{k+1})} \sum_{j=n-1}^{k-1} 2q_j(p_{k+1}) \\ &\times \mathrm{cov}[\tau_{k-1}, h_j] \quad (n \leq k, n \geq 2) \\ &\mathrm{cov}[\tau_n, h_k] = \frac{\sigma_{\tau_{k+1}}^2}{2q_k(p_{k+1})} \quad (n = k+1) \\ &\mathrm{cov}[\tau_n, h_k] = 0 \qquad (n \geq k+2) \end{aligned}\right\}. \tag{13}$$

We can evaluate the error in depth estimates using Equations (9) through (13).

Estimated errors in the P-wave velocity function (Figure 4, east side) are shown in Figure 11. The magnitude of all measurement errors in $\tau(\sigma_\tau)$ are assumed to be 0.05 s. The τ-p data used for estimating errors were more sparsely picked from the P-wave τ-p trajectory of Figure 2 than those used to derive the velocity structure due to computer per-

formance restrictions. The estimated errors in depths are a few hundred meters at shallow depths and 300 ~ 500 m in the deeper crust. At depths greater than 1 km, the accuracy of $V(d)$ function decreases slightly. In interpreting Figure 11, one should bear in mind that the depth errors where velocity increases rapidly will be large (e.g., at the sediment-basement interface), and if one misreads a part of the τ-p trajectory, the corresponding errors become large. These effects, however, are localized and have little affect on depth estimates for larger velocities.

Conclusions

The τ-p method is useful for high resolution analysis of OBS records to determine the seismic velocity structure in shallow oceanic crust. The derived $V(d)$ functions are consistent with velocities of both core samples and sonic logs at the ODP holes in the vicinity of the OBS. The derived P- and S-wave velocity functions also agree with coincident seismic reflection profile data and rapid velocity increases corresponds to observed reflectors. We also obtain interface dip angles and true velocities in each layer by using split-spread profile records. In addition, we developed the method to estimate depth errors in the velocity functions. The estimated errors of the derived $V(d)$ function in shallow crust are comparable to the seismic source wave length of 150 m, indicating that the τ-p method is a method with approximately three times higher resolution in comparison with conventional OBS velocity analysis methods for shallow oceanic crust. The higher resolution depends on accurate positioning of shots determined by GPS, spatially dense seismic observations and the use of unsaturated reflected waves that arrive after the direct water wave observed on low-gain component records. Improved higher quality seismic observations depend upon the development of OBS's with increased sensitivity and a wider dynamic range. The τ-p method has computational and interpretational advantages and leads directly to a detailed velocity function versus depth. Use of seismic sources that produce a higher frequency seismic wave (e.g., watergun) and digital OBS's with wider dynamic ranges will allow us to obtain higher resolution $V(d)$ function. Increasing the spatial density of accurately positioned observation will also help to provide higher resolution $V(d)$ function for OBS records. Results with up to four times higher resolution than previous results can be obtained by using waterguns that produce a seismic source with a dominant frequency of about 40 Hz instead of airguns.

Acknowledgements

We thank Y. Ono and K. Hayashi for discussions and providing computer programs. We also thank K. Suyehiro and A. Klaus for critical reading of the manuscript, and S. Kuramoto for providing core sample and sonic logging data. Comments by J. B. Diebold and an anonymous reviewer helped us improve the manuscript. Parts of the computations were performed at Chiba University, Information Processing Center and at Ocean Research Institute, the University of Tokyo.

References

Bessonova, E. N., Fishman, V. M., Pyaboyi, V. Z., and Sitnikova, G. A., 1974, The Tau-Method for Inversion of Travel Time — I. Deep Seismic Sounding Data, *Geophys. J. R. Astron. Soc.* **36**, 377–398.

Červený, V., Molotkov, I. A., and Pšenčik, I., 1977, *Ray Method in Seismology*, Univerzita Karlova, Prague, p. 215.

Diebold, J. B. and Stoffa, P. L., 1981, The Traveltime Equation, Tau-p Mapping, and Inversion of Common Midpoint Data, *Geophysics* **46**, 238–254.

Diebold, J. B., 1989, Tau-p Analysis in One, Two and Three Dimensions. In Stoffa, P. L. (ed.), *Tau-p: A Plane Wave Approach to the Analysis of Seismic Data*, Kluwer Academic Publishers, Dordrecht, pp. 71–118.

Henry, M, Orcutt, J. A., and Parker, R. L., 1980, A New Method for Slant Stacking Refraction Data, *Geophys. Res. Let.* **7**, 1073–1076.

Kappus, M. E., Harding, A. J., and Orcutt, J. A., 1990, A Comparison of Tau-p Transform Methods, *Geophysics* **55**, 1202–1215.

Milkereit, B., Mooney, W. D., and Kohler, W. M., 1985, Inversion of Seismic Refraction Data in Planar Dipping Structure, *Geophys. J. R. Astron. Soc.* **82**, 81–103.

Neidell, N. S. and Taner, M. T., 1971, Semblance and Other Coherency Measures for Multichannel Data, *Geophysics* **36**, 483–497.

Nishizawa, A. and Suyehiro, K., 1986, Crustal Structure Across the Kurile Trench off Southeastern Hokkaido by Airgun-OBS Profiling, *Geophys. J. R. Astron. Soc* **86**, 371–397.

Shinohara, M., Hirata, N., Nambu, H., Suyehiro, K., Kanazawa, T., and Kinoshita, H., 1992, Detailed Crustal Structure of Northern Yamato Basin. In Tamaki, K., Suyehiro, K., Allan, J., McWilliams, M. *et al.* (eds.), *Proc. ODP., Sci. Results.* **127/128**, Pt2, 1075–1106, College Station, TX (Ocean Drilling Program).

Shipboard Scientific Party, 1990a, Site 794, In Tamaki, K., Allan, J. *et al.* (eds.), *Proc. ODP. Init. Repts.* **127**, 71–167, College Station, TX (Ocean Drilling Program).

Shipboard Scientific Party, 1990b, Site 794, In Ingle, J. C., Jr., Suyehiro, K., von Breymann, M. T. *et al.* (eds.), *Proc. ODP. Init. Repts.* **128**, 67–120., College Station, TX (Ocean Drilling Program).

Stoffa, P. L., Buhl, P., Diebold, J. B., and Wenzel, F., 1981, Direct Mapping of Seismic Data to the Domain of Intercept Time and Ray Parameter – A Plane-Wave Decomposition, *Geophysics* **46**, 255–267.